Natural Compounds as Ferroptosis Inducers

Subjects: Pharmacology & Pharmacy

Contributor: Carmela Fimognari , Greco Giulia

Ferroptosis is classified as a non-canonical cell death mechanism. To date, several natural compounds have been discovered to induce ferroptosis in different cancer models.

non-canonical cell death ferroptosis natural compounds

1. Ferroptosis

Ferroptosis, firstly discovered by Dixon et al. in 2012 [1], is a non-canonical cell death characterized by an iron-dependent accumulation of lipid reactive oxygen species (ROS), which leads to cell demise [2]. Ferroptosis differs from any other form of regulated cell death. Morphologically, it does not involve any typical apoptotic feature; it is not characterized by cytoplasmatic swelling or disruption of cell membrane, as in necrotic cell death; the formation of typical autophagic vacuoles is not observed [1]. Ferroptotic cells, instead, are morphologically characterized by a distinct shrinkage of mitochondria with enhanced membrane density and decrease/depletion of mitochondrial cristae [1].

Ferroptosis is caused by compounds able to antagonize glutathione peroxidase 4 (GPX4) in a direct way or through the inhibition of X_c^- system. X_c^- system is an amino acid antiporter responsible for intracellular transport of extracellular cystine by exchanging intracellular glutamate [3] (Figure 1). Once inside the cells, cystine is reduced to cysteine, an essential substrate for glutathione (GSH) synthesis [4]. Hence, the inhibition of X_c^- system alters GSH biosynthesis, reducing the antioxidant activity of glutathione and selenium-dependent GPXs [5][6][7]. Among GPXs, GPX4 is the only one able to reduce hydrogen peroxides or organic hydroperoxides into water or corresponding alcohols by converting GSH into oxidized glutathione (GSSG) [8][9] (Figure 1). Then, the inhibition of GPX4, through direct or indirect mechanisms, leads to lipid ROS accumulation and activates the ferroptotic cell death cascade [1][10][11] (Figure 1).

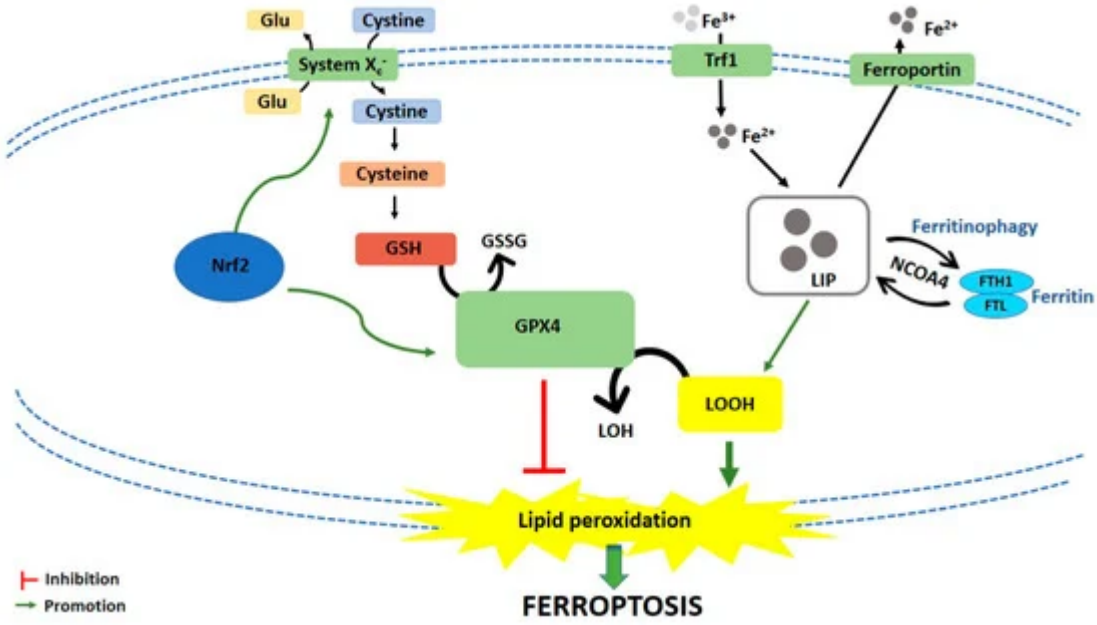

Figure 1. Schematic representation of ferroptotic cell death pathway. Glu: Glutamate; GSH: Glutathione; GSSG: Oxidized glutathione; GPX4: Glutathione peroxidase 4; LOH: Lipid alcohols; LOOH: Lipid hydroperoxides; Nrf2: Nuclear factor (erythroid-derived 2)-like 2; Trf1: Transferrin receptor 1; LIP: Labile iron pool; FTH1: Ferritin heavy chain 1; FTL: Ferritin light chain; NCOA4: Nuclear receptor coactivator.

Iron-dependent accumulation of lipid ROS can occur through non-enzymatic and/or enzymatic lipid peroxidation. Non-enzymatic lipid peroxidation, also called lipid autoxidation, consists in a free radical-driven chain reaction where ROS initiate the oxidation of polyunsaturated fatty acids (PUFAs). Within an autocatalytic process, autoxidation can be propagated leading to membrane destruction, and subsequent ferroptotic cell death [12]. Enzymatic lipid peroxidation is mostly driven by lipoxygenases (LOXs). LOXs, through their dioxygenase activity, catalyze oxygen insertion into PUFAs membrane, generating different lipid hydroperoxides (LOOH), which can start the autocatalytic process of lipid autoxidation mentioned above [11].

If the link between lipid metabolism and ferroptosis induction is well known, how lipid peroxidation leads to ferroptotic cell death is not clear yet. Two mechanisms have been hypothesized. The first hypothesis is that lipid hydroperoxides, produced by PUFAs peroxidation, generate reactive toxic products, i.e., 4-hydroxy-2-nonenal (4-HNE) or malondialdehyde (MDA), which consequently inactivate different survival proteins, leading to ferroptosis [13]. The second hypothesis is that extensive phospholipids peroxidation leads to structural and functional modifications of cellular membrane [12].

2. Natural Compounds as Ferroptosis Inducers

Several natural compounds, alone or in combination, have been found to induce ferroptosis in different in *vitro* cancer models (Table 1).

Table 1. Natural products as in vitro inducers of ferroptosis.

Compound	Compound Source	Cell Line(s)	Concentrations (Where Specified)	Time (Where Specified)	Ferroptosis Markers	Supplementary Effects
Actinia chinensis (Planch), drug-containing rat serum	*Actinia chinensis* Planch	HGC-27	90, 180 and 360 mg/mL	48 h	↓ Cell proliferation	
				24 and 48 h	↓ Cell migration	
			180 mg/mL	48 h	↑ ROS	↓ after Ferr-1 treatment
			90, 180 and 360 mg/mL		↓ GPX4	
					↓ xCT	
Albiziabioside A	*Albizia inundata* Mart.	MCF-7	10 μM	24 h	↑ Cytotoxicity	↑ after Fe^{2+} treatment
						↓ after Ferr-1 treatment
						↓ after DFO treatment
						↓ after vitamin E treatment
				/	↑ ROS	
				24 h	↓ GSH/GSSG ratio	
				48 h	↓ GPX4 protein expression	
				/	↑ MDA	
					↑ Lipid peroxides	
Amentoflavone	*Selaginella* spp. and other plants	U251, U373	10 and 20 μM	/	↑ Fe^{2+}	
					↓ FTH	↑ after ATG7 knockdown
					↑ MDA	↓ after FTH overexpression

Compound	Compound Source	Cell Line(s)	Concentrations (Where Specified)	Time (Where Specified)	Ferroptosis Markers	Supplementary Effects
						↓ after FTH overexpression
					↑ Lipid ROS	↓ after BafA1 treatment
						↓ after ATG7 knockdown
						↓ after FTH overexpression
					↓ GSH	↓ after BafA1 treatment
						↓ after ATG7 knockdown
						↓ after Ferr-1 treatment
						↓ after DFO treatment
Ardisiacrispin B	*Ardisia kivuensis* Taton	CCRF-CEM	20 μM	24 h	↑ Cell death ratio (%)	↓ after FTH overexpression
						↓ after BafA1 treatment
						↓ after ATG7 knockdown
						↓ after Ferr-1 treatment
						↓ after DFO treatment
			0.59, 0.93, 2.33, 4.66, 9.32, 18.64 and 37.28 μM		↑ Cytotoxicity	
			0.3, 0.6, 1.2 and 2.4 μM		↑ ROS	
Aridanin	*Tetrapleura tetraptera* (Schum. & Thonn) Taub.	CCRF-CEM	1, 2, 4, 8, 15, 30 and 61 μM	24 h	↓ Cell viability	↓ after Ferr-1 treatment
						↓ after DFO treatment

Compound	Compound Source	Cell Line(s)	Concentrations (Where Specified)	Time (Where Specified)	Ferroptosis Markers	Supplementary Effects
Artenimol (artemisinin semi-syntethic derivative)	*Artemisia annua* L.	CCRF-CEM	0.01, 0.1, 1, 10 and 100 μM	/	↓ Cell viability	↓ after Ferr-1 treatment
						↓ after DFO treatment
Artesunate (artemisin semi-synthetic derivative)	*Artemisia annua* L.	DAUDI, CA-46	4 and 20 μM	48 h	↓ Cell viability	↑ after DFO treatment
						↑ after Ferr-1 treatment
						↑ after Lip-1 treatment
						↑ after down-regulation of CHAC1 expression
			5, 10 and 20 μM	24 and 48 h	↑ ROS	
					↑ Lipid peroxidation	↓ after down-regulation of CHAC-1 expression
			5, 10 and 20 μM	24 h	↑ CHAC1, ↑ ATF4, ↑ CHOP protein expression	
		MT-2	50 μM	24 h	↑ ROS	
			0.4, 2 and 10 μM		↑ Cytotoxicity	↓ after DFO treatment
			2 and 10 μM			↓ after Ferr-1 treatment
		HUT-102	50 μM	24 h	↑ ROS	↓ after NAC treatment
			2 and 10 μM		↑ Cytotoxicity	↓ after DFO treatment

Compound	Compound Source	Cell Line(s)	Concentrations (Where Specified)	Time (Where Specified)	Ferroptosis Markers	Supplementary Effects
			10 and 50 μM			↓ after Ferr-1 treatment
			50 μM			↓ after HTF treatment
						↑ after DFO treatment
				72 h	↓ Cell viability	↑ after Trolox treatment
		HN9	2.5 and 5 μM			↑ after Keap1 knockdown
						↑ after Nrf2 knockdown
					↑ ROS	↓ after Ferr-1 treatment
						↓ after Trolox treatment
			50 μM	24 h		↓ after Ferr-1 treatment
					↑ Lipid ROS	↓ after Trolox treatment
					↑ Nrf2 protein expression	
		HN9, HN9-cisR	10, 25 and 50 μM	24 h	↓ xCT, ↓ RAD51, ↓ Keap1 protein expression	
		HN9-cisR, HN3-cisR, HN4-cisR	10, 25 and 50 μM	24 h	↑ Nrf2, ↑ HO-1, ↑ NQO1 protein expression	
					↓ Keap1 protein expression	

Compound	Compound Source	Cell Line(s)	Concentrations (Where Specified)	Time (Where Specified)	Ferroptosis Markers	Supplementary Effects
			50 μM		↑ Nrf2, ↑ HO-1, ↑ NQO1 mRNA levels	
						↓ after trigonellin treatment
					↓ GSH	↑ after Trolox treatment
						↑ after Nrf2 knockdown
					↑ ROS	↓ after Trolox treatment
		HN3-cisR	25 and 50 μM	24 h		↑ after Nrf2 knockdown
					↑ Lipid ROS	↓ after trigonellin treatment
						↓ after Nrf2 knockdown
					↓ Cell viability	↓ after HO-1 knockdown
						↑ after Trolox treatment
		PaTU8988, AsPC-1	20 μM	24 h		↑ after Ferr-1 treatment
					↓ Cell viability	↑ after GRP78 overexpression
						↓ after GRP78 knockdown
					↑ MDA	↓ after DFO treatment
						↓ after Ferr-1 treatment

Compound	Compound Source	Cell Line(s)	Concentrations (Where Specified)	Time (Where Specified)	Ferroptosis Markers	Supplementary Effects
						↓ after GRP78 overexpression
						↑ after GRP78 knockdown
					↑ Lipid peroxidation	↓ after Ferr-1 treatment
			10, 20 and 40 μM		↑ GRP78 mRNA levels	
					↑ GRP78 protein expression	
		HEY1	25 and 50 μM	48 h	↑ Cell death	↓ after Ferr-1 treatment
						↓ after DFO treatment
						↑ after HT treatment
		HEY2	100 μM		↑ Cell death	↓ after Ferr-1 treatment
		HEY2, SKOV3	50 and 100 μM		↑ Cell death	↓ after DFO treatment
						↑ after HT treatment
		HEY1, HEY2, SKOV-3	10, 25, 50 and 100 μM	24 h	↑ ROS	↓ after GSH treatment
		HEY1, HEY2, SKOV-3, OVCAR8, TOV-112D, TOV-21G	25, 50 and 100 μM	48 h	↑ Cell death	↓ after GSH treatment
		Panc-1	50 μM	24 h	↑ ROS	↓ after Trolox treatment

Compound	Compound Source	Cell Line(s)	Concentrations (Where Specified)	Time (Where Specified)	Ferroptosis Markers	Supplementary Effects
						↑ after DFO treatment
					↓ Colony formation	↑ after Trolox treatment
						↑ after Ferr-1 treatment
						↓ after HTF treatment
					↑ HO-1 protein expression	
					↑ Lipid peroxidation	↓ after Trolox treatment
						↓ after Ferr-1 treatment
		Panc-1, COLO-357		48 h	↑ Cell death	↓ after Ferr-1 treatment
		BxPC-3, Panc-1		24 and 48 h	↑ Cell death	↓ after DFO treatment
		BxPC-3, Panc-1, AsPC-1			↑ Cell death	↑ after HTF treatment
Betula etnensis Raf. methanolic extract	*Betula etnensis* Raf.	CaCo2	5, 50, 250 and 500 µg/mL	72 h	↓ Cell viability	
			5, 50 and 250 µg/mL		↑ LDH release	
					↑ ROS	
					↑ LOOH	
					↓ RSH	
			5 and 50 µg/mL		↓ HO-1 levels	

Compound	Compound Source	Cell Line(s)	Concentrations (Where Specified)	Time (Where Specified)	Ferroptosis Markers	Supplementary Effects
			250 μg/mL		↑ HO-1 levels	
D13 (albiziabioside A derivative)	*Albizia inundata* Mart.	HCT116	0.31, 1.25 and 5 μM	/		↓ after Ferr-1 treatment
						↓ after DFO treatment
					↑ Cytotoxicity	↑ after Fe^{2+} treatment
						↑ after Fe^{3+} treatment
				48 h	↓ GPX4 protein expression	
Dihydroartemisinin (artemisin semi-synthetic derivative)	*Artemisia annua* L.	THP-1	5, 10 and 15 μM	/	↑ MDA	
				12 h	↓ Cell viability	
					↑ ROS	
		HL-60	5, 10 and 15 μM	12 h	↓ Cell viability	↑ after Ferr-1 treatment
						↑ after DFO treatment
						↑ after NAC treatment
						↑ after BafA1 treatment
						↑ after 3-MA treatment
						↑ after ATG7 knockdown
						↑ after FTH overexpression

Compound	Compound Source	Cell Line(s)	Concentrations (Where Specified)	Time (Where Specified)	Ferroptosis Markers	Supplementary Effects
						↑ after ISCU overexpression
					↑ Lipid ROS	↓ after ATG7 knockdown
						↓ after FTH overexpression
					↓ GSH	↑ after ISCU overexpression
					↑ ROS	↓ after DFO treatment
						↓ after NAC treatment
						↓ after ISCU overexpression
					↑ IRP2 protein expression	
					↓ FTH, ↓ GPX4 protein expression	↑ after ISCU overexpression
						↑ after BafA1 treatment
		G0101, G0107	10, 20, 40, 80 and 160 μM	24 h	↑ ROS	
			20, 40, 80 and 160 μM		↑ Lipid ROS	
					↑ MDA	
					↓ GSH	
					↑ GSSG	
					↑ Cell death	↓ after DFO treatment
						↓ after Ferr-1 treatment

Compound	Compound Source	Cell Line(s)	Concentrations (Where Specified)	Time (Where Specified)	Ferroptosis Markers	Supplementary Effects
						↓ after Lip-1 treatment
		U251 U373	5, 10, 20 and 40 μM 20, 40, 80 and 160 μM	24 h	↓ GSH	
						↓ after DFO treatment
		U251 U373	2.5, 5, 10, 20 and 40 μM 10, 20, 40, 80 and 160 μM	24 and 48 h	↑ ROS	↑ after PERKi treatment
						↑ after ATF4 siRNA treatment
						↑ after HSPA5 siRNA treatment
		U251 U373	2.5, 5, 10 and 20 μM 10, 20, 40, 80 and 160 μM	3, 6, 12, 24 and 48 h	↑ Lipid ROS	↑ after ATF4 siRNA treatment
						↑ after HSPA5 siRNA treatment
						↑ after PERKi treatment
		U251 U373	5, 10, 20 and 40 μM 80 μM	3, 6, 12, 24 and 48 h	↑ MDA	↑ after ATF4 siRNA treatment
						↑ after HSPA5 siRNA treatment
		U251 U373	10, 20 and 40 μM 40, 80 and 160 μM	48 h	↑ Cell death	↓ after DFO treatment
						↓ after Ferr-1 treatment

Compound	Compound Source	Cell Line(s)	Concentrations (Where Specified)	Time (Where Specified)	Ferroptosis Markers	Supplementary Effects
						↓ after Lip-1 treatment
						↑ after PERKi treatment
						↑ after ATF4 siRNA treatment
						↑ after HSA5 siRNA treatment
Dihydroisotanshinone I	*Salvia miltiorrhiza* Bunge	MCF-7	5 and 10 μM	24 h	↓ GPX4 activity	
		MCF-7, MDA-MB231	10 μM		↓ GPX4 protein expression	
			5 and 10 μM		↑ MDA	
			10 μM		↓ GSH/GSSG ratio	
Epunctanone	*Garcinia epunctata* Stapf.	CCRF-CEM	1.04, 1.66, 4.14, 8.28, 16.56, 33.11 and 66.23 μM	24 h	↑ Cytotoxicity	↓ after Ferr-1 treatment
						↓ after DFO treatment
			2.95, 5.91, 11.81 and 23.63 μM		↑ ROS	
Erianin	*Dendrobium chrysotoxum* Lindl	H460, H1299	50 and 100 nM	24 h	↑ Cell death	↓ after NAC treatment
						↓ after Ferr-1 treatment
						↓ after Lip-1 treatment
						↓ after GSH treatment

Compound	Compound Source	Cell Line(s)	Concentrations (Where Specified)	Time (Where Specified)	Ferroptosis Markers	Supplementary Effects
Ferroptocide (pleuromutilin semi-syntetic derivative)	*Pleurotus passeckerianus; Drosophila subatrata; Clitopilus scyphoides,* and others spp.	ES-2	50 and 100 nM		↑ ROS	
					↓ GSH	
					↑ MDA	
			12.5, 25, 50 and 100 nM	/	↑ HO-1, ↑ transferrin protein expression	
					↓ GPX4, ↓ CHAC2, ↓ SLC40A1, ↓ SLC7A11 protein expression	
			5, 10 and 25 μM	24 h	↑ Ca^{2+} levels	
					↑ Calmodulin protein expression	
			5, 10 and 25 μM		↑ ROS	↓ after DFO treatment
			10 and 25 μM	1 h	↑ Mitochondrial ROS	
			10 μM		↑ Lipid ROS	↓ after DFO treatment
		HCT116		14 h		↓ after Ferr-1 treatment
			5, 10 and 25 μM		↑ Cell death	↓ after DFO treatment
						↓ after Trolox treatment
			5, 10 and 25 μM	10, 24 and 48 h	↑ Cell death	↓ after DFO treatment
						↓ after Trolox treatment

Compound	Compound Source	Cell Line(s)	Concentrations (Where Specified)	Time (Where Specified)	Ferroptosis Markers	Supplementary Effects
						↓ after NAC-1 treatment
						↑ after TXN knockdown
						↓ after Ferr-1 treatment
			5, 10 and 25 μM	1.5 and 72 h	↑ ROS	↑ after TXN knockdown
			10 μM	2 and 72 h	↑ Lipid ROS	↑ after TXN knockdown
						↓ after DFO treatment
		4T1	5, 10 and 25 μM	18 h	↑ Cell death	↓ after DFO treatment
						↓ after Ferr-1 treatment
			10 μM	2 h	↑ Lipid ROS	↓ after Ferr-1 treatment
						↓ after DFO treatment
		HT-29	5, 10 and 25 μM	12 h	↑ Cell death	↓ after DFO treatment
						↓ after Trolox treatment
						↓ after NAC treatment
						↓ after Ferr-1 treatment
Gallic Acid	Natural polyhydroxy phenolic compound, found in various foods	HeLa	50 μg/mL	12 h	↑ Lipid peroxidation	
		HeLa, H446, SHSY-5Y		36 h	↑ Cell death	↓ after DFO treatment

Compound	Compound Source	Cell Line(s)	Concentrations (Where Specified)	Time (Where Specified)	Ferroptosis Markers	Supplementary Effects
		A375, MDA-MB-231	10, 25, 50, 100 and 200 μg/mL		↓ Cell viability	
		MDA-MB-231	25 μg/mL	24 h	↑ ROS	
		A375	50 μg/mL			
		MDA-MB-231	/	/	↓ GPX4 activity	
		A375, MDA-MB-231	/	/	↑ MDA	
Physcion 8-O-β-glucopyranoside	*Rumex japonicus* Houtt.	MGC-803, MKN-45				↑ after Ferr-1 treatment
			10, 20, 30, 40 and 50 μM	24, 48, 72 and 96 h	↓ Cell viability	↑ after GPNA treatment
						↑ after 968 treatment
						↓ after GLS2 knockdown
			/	/	↓ Cell proliferation	↑ after miR-103a-3p overexpression
			/	24 h	↓ Cell invasion	↑ after miR-103a-3p overexpression
					↓ Cell migration	↑ after miR-103a-3p overexpression
			/	/	↑ Lipid ROS	↓ after GPNA treatment
						↓ after 968 treatment
						↓ after GLS2 knockdown

Compound	Compound Source	Cell Line(s)	Concentrations (Where Specified)	Time (Where Specified)	Ferroptosis Markers	Supplementary Effects
						↓ after miR-103a-3p overexpression
						↓ after GPNA treatment
						↓ after 968 treatment
					↑ MDA	↓ after GLS2 knockdown
						↓ after miR-103a-3p overexpression
						↓ after GPNA treatment
						↓ after 968 treatment
					↑ Fe^{2+}	↓ after GLS2 knockdown
						↓ after miR-103a-3p overexpression
					↓ miR-103a-3p expression	
					↑ GLS2 protein levels	↓ after miR-103-3p transfection
Piperlongumine	*Piper Longum* L.	Panc-1	4, 6, 8, 10, 12 and 14 μM	16 h	↓ Cell viability	↑ after NAC treatment
						↑ after Ferr-1 treatment
						↑ after Lip-1 treatment

Compound	Compound Source	Cell Line(s)	Concentrations (Where Specified)	Time (Where Specified)	Ferroptosis Markers	Supplementary Effects
						↑ after DFO treatment
		MIAPaCa-2	10 μM [14]	16 h	↓ Cell viability	↑ after CPX treatment [15][16][17][18][19][20]
[21]						↑ after PD146176 treatment
				4 h	↓ GSH	
Progenin III	*Raphia vinifera* P. Beauv	CCRF-CEM	2, 3, 7, 14 and 55 μM	24 h	↓ Cell viability	↑ after Ferr-1 treatment ↑ after DFO treatment
			1.59 and 3.18 μM		↑ ROS [15]	
			7 μM [22][23][24]	/	↑ Cell death	↑ after FAC treatment ↓ after DFO treatment
Ruscogenin	*Ruscus aculeatus* L. *Radix Ophiopogon* [26][27] *japonicas* (Thunb.) Ker Gawl.	BxPC-3, SW1990	/	6 h [26]	↑ Cell death	↑ after transferrin knockdown [25] ↓ after ferroportin overexpression [27]
			3 and 7 μM	12 and 24 h	↑ Fe^{2+} [26][27]	↓ after DFO treatment
		nu +		1, 2, 4, 6 and 24 h	↑ ROS	↓ after DFO treatment
[28]			6 and 12 μM	24 h	↑ Transferrin ↓ Ferroportin	
Solasonine	*Solanum melongena* L. [32]	HepG2	15 ng/mL	24 h [33]	↑ Cell death	↓ after Fer-1 treatment [29][30]

[31]

the modulation of different molecular targets (Table 1). One of these targets is the endoplasmic reticulum (ER). ER stress is a condition of oxidative stress and perturbations in the ER folding machinery provoked by the accumulation of unfolded/misfolded proteins. ER stress activates a signaling process, called unfolded protein response (UPR), in order to lessen ER stress and to restore ER homeostasis [34][35]. In DAUDI and CA-46 lymphoma cells, artesunate triggered ferroptosis and ER stress through the activation of ATF4 (activating transcription factor-4)-CHOP (C/EBP [CCAAT-enhancer-binding protein] homologous protein)-CHAC1 (glutathione-

Compound	Compound Source	Cell Line(s)	Concentrations (Where Specified)	Time (Where Specified)	Ferroptosis Markers	Supplementary Effects
[36]		[36]		[36]		
[37][38]				[36]		↓ after DFO treatment
					cellular cystein	
					↑ Lipid ROS	↓ after Ferr-1 treatment
						↓ after DFO treatment
[29]						
				[39]	↓ GSS, ↓ GPX4 mRNA levels [40]	
		[29]				
				[30]	↓ GSS, ↓ GPX4 protein expression	
Typhaneoside	*Pollen Typhae*	Kas-1, HL-60, NB4	[32][41]	24 h		↑ after Ferr-1 treatment
		[32][42][43]				↑ after DFO treatment
						↑ after 3-MA treatment
			[44][45][46] 40 μM		↓ Cell viability [49][50][51]	↑ after BafA1 treatment
		[47][48]				↑ after Z-VAD-FMK treatment
	[44][52][53]					↑ after rapamycin treatment [54]
					[55][56][57]	↑ after ATG7 knockdown
			20, 30 and 40 μM		↑ ROS	↓ after DFO treatment
						↓ after NAC treatment [58]
[58]					↓ GSH	
			[58]			

often leads to low antioxidant ferritin and transferrin levels and increased pu

ranch of
radation
F4 could
rroptosis
ma cells
-induced
BALB/c
ered the
RK, IRE1
-induced
t way in
c cancer
mutation
and may
e hardly

ally, Nrf2
nditions,
tioxidant
d in the
iron and
chain of
egulator
re, since
tion and
ught that
ay could
ability in
or heme
tioxidant
Kwon et
ced lipid

f2 in ferroptosis seems to be cell-type specific [91], since the activation of Nrf2 pathway protected hepatocellular carcinoma cells against ferroptosis [55], while it promoted ferroptosis in neuroblastoma [59]. Taken together, those results support the hypothesis that Nrf2 could act as a double-edge sword. Even if further studies are needed to disentangle this knot, artesunate supports this hypothesis inducing different effects in different cell lines.

Compound	Compound Source	Cell Line(s)	Concentrations (Where Specified)	Time (Where Specified)	Ferroptosis Markers	Supplementary Effects
[32]	[30]		[32]	[32]	↑ Lipid ROS	↓ after ATG7 knockdown
						↓ after BafA1 treatment
					↓ GPX4, ↓ FTH mRNA levels	
					↑ IRP2 mRNA levels	
Ungeremine [60]	*Crinum zeylanicum* L. [60]	CCRF-CEM	2.37, 3.76, 9.40, 18.79, 37.58, 75.17 and 150.33 μM	24 h	↓ Cell proliferation	↑ after Ferr-1 treatment
						↑ after DFO treatment
			1.22, 2.45, 4.89 and 9.78 μM		↑ ROS	
Whitaferin A [59]	*Withania somnifera* (L.) Dunal	IMR-32 [59]	/	/	↑ ROS	
			1 and 10 μM	2, 4, 8, 12 and 24 h	↓ GPX4 expression	
		[59]	10 μM	3 and 5 h	↓ GPX4 activity	
		[59]	/ [59]	/	↑ Lipid peroxidation	↓ after DFO treatment
			1 μM	4, 8 and 12 h	[59] ↑ Fe^{2+}	↑ after hemin treatment
				[61] 1, 2, 4, 8, 12 and 24 h	↑ HO-1, ↑ Keap1, ↑ Nrf2 protein expression	
				6, 8, 12 and 16 h	↑ Cell death [59]	↓ after GPX4 overexpression
				[59]		↓ after ZnPP treatment

References

1. Dixon, S.J.; Lemberg, K.M.; Lamprecht, M.R.; Skouta, R.; Zaitsev, E.M.; Gleason, C.E.; Patel, D.N.; Bauer, A.J.; Cantley, A.M.; Yang, W.S.; et al. Ferroptosis: An Iron-Dependent Form of Nonapoptotic Cell Death. Cell 2012, 149, 1060–1072, doi:10.1016/j.cell.2012.03.042.

Compound	Compound Source	Cell Line(s)	Concentrations (Where Specified)	Time (Where Specified)	Ferroptosis Markers	Supplementary Effects
						↓ HO-1 knockdown
						↑ after hemin treatment
						↓ after Ferr-1 treatment
						↓ after CPX treatment
			1 and 10 μM	6, 8, 12 and 16 h	↑ Cell death	↓ after α-tocopherol treatment
						↓ after UOI26 treatment
		IMR-32, SK-N-SH				↓ after Flt3 inhibitor treatment
				/	Nrf2 pathway activation	
			1 μM	/	↑ FTH1, ↑ HO-1 gene expression	
				1, 2, 4, 8, 12 and 24 h	↑ FTH1, ↑ HO-1 mRNA levels	
WA-NPs	*Withania somnifera* L. Dunal	IMR-32	1 and 10 μM	8, 10, 12, 16, 20 and 24 h	↑ Cell death	

Abbreviations: ↑: Increase; ↓: Decrease; 3-MA:3-methyladenine; 968: Compound 968, GLS2 inhibitor;; ATF4: Activating transcription factor 4; ATG7: Autophagy related 7; BafA1: Bafilomycin 1; CHAC1: Glutathione-specific Gamma-glutamylcyclotransferase 1; CHOP: CCAAT/enhancer-binding protein homologous protein; CPX: Ciclopirox; intracellular iron chelator; DFO: Deferoxamine; FAC: Ferric ammonium citrate; Fe^{2+}: Ferrous ion; Fe^{3+}: Ferric ion; Ferr-1: Ferrostatin-1; Flt3: Receptor tyrosine kinase fms-like tyrosine kinase 3; FTH: Ferritin heavy chain; FTH1: Ferritin heavy chain 1; GLS2: Glutaminase 2; GPNA: Glutamine transporter inhibitor; GPX4: Glutathione peroxidase IV; GSH: Glutathione; GSS: Glutathione synthetase; GSSG: Oxidized glutathione; HO-1:

Cheah, J.H.; Clemons, P.A.; Shamji, A.F.; Clish, C.B.; et al. Regulation of Ferroptotic Cancer Cell Death by GPX4. Cell 2014, 156, 317–331, doi:10.1016/j.cell.2013.12.010.

11. Yang, W.S.; Kim, K.J.; Gaschler, M.M.; Patel, M.; Shchepinov, M.S.; Stockwell, B.R. Peroxidation of Polyunsaturated Fatty Acids by Lipoxygenases Drives Ferroptosis. Proc. Natl. Acad. Sci. USA 2016, 113, E4966–4975, doi:10.1073/pnas.1603244113.

12. Feng, H.; Stockwell, B.R. Unsolved Mysteries: How Does Lipid Peroxidation Cause Ferroptosis? PLoS Biol. 2018, 16, e2006203, doi:10.1371/journal.pbio.2006203.

13. Ayala, A.; Muñoz, M.F.; Argüelles, S. Lipid Peroxidation: Production, Metabolism, and Signaling Mechanisms of Malondialdehyde and 4-Hydroxy-2-Nonenal. Oxidative Med. Cell Longev. 2014, 2014, 360438, doi:10.1155/2014/360438.

Heme oxygenase 1; H3-cisR: Cisplatin-resistant H3 cells; H4-cisR: Cisplatin-resistant H4 cells; H19-cisR: Cisplatin-resistant H19 cells; HSPA5: Heat shock protein family A (Hsp70) member 5; HTF: Holo-transferrin; IRP2: Iron regulatory protein 2; ISCU: Iron-sulfur cluster assembly enzyme; Keap1: Kelch-like ECH-associated protein 1; Lip-1: Liproxstatin-1; MDA: Malondialdehyde; NAC: N-acetylcysteine; NQO1: NAD(P)H quinone dehydrogenase 1; Nrf2: Nuclear factor erythroid 2–related factor 2; PD146176: Lypoxygenase inhibitor; PERKi: PERK inhibitor I (GSK2606414); ROS: Reactive oxygen species; RSH: Thiols; Spp.: Species; TXN: Thioredoxin; WA-NPs: Whitaferin A nanoparticles; xCT: Cystine/glutamate antiporter; ZnPP: Zinc protoporphyrin, HO-1 inhibitor; Z-VAD-FMK: Pan-caspase inhibitor.

14. Yu, S.; Yan, H.; Zhang, L.; Shan, M.; Chen, P.; Ding, A.; Li, S. A Review on the Phytochemistry, Pharmacology, and Pharmacokinetics of Amentoflavone, a Naturally-Occurring Biflavonoid. Molecules 2017, 22, 299, doi:10.3390/molecules22020299.

15. Chen, Y.; Li, N.; Wang, H.; Wang, N.; Peng, H.; Wang, J.; Li, Y.; Liu, M.; Li, H.; Zhang, Y.; et al. Amentoflavone Suppresses Cell Proliferation and Induces Cell Death through Triggering Autophagy-Dependent Ferroptosis in Human Glioma. Life Sci. 2020, 247, 117425, doi:10.1016/j.lfs.2020.117425.

16. Lee, J.S.; Lee, M.S.; Oh, W.K.; Sul, J.Y. Fatty Acid Synthase Inhibition by Amentoflavone Induces Apoptosis and Antiprolifer-ation in Human Breast Cancer Cells. Biol. Pharm. Bull. 2009, 32, 1427–1432, doi:10.1248/bpb.32.1427.

17. Lee, K.-C.; Tsai, J.-J.; Tseng, C.-W.; Kuo, Y.-C.; Chuang, Y.-C.; Lin, S.-S.; Hsu, F.-T. Amentoflavone Inhibits ERK-Modulated Tumor Progression in Hepatocellular Carcinoma in Vitro. Vivo 2018, 32, 549–554, doi:10.21873/invivo.11274.

18. Chiang, C.-H.; Yeh, C.-Y.; Chung, J.G.; Chiang, I.-T.; Hsu, F.-T. Amentoflavone Induces Apoptosis and Reduces Expression of Anti-Apoptotic and Metastasis-Associated Proteins in Bladder Cancer. Anticancer Res. 2019, 39, 3641–3649, doi:10.21873/anticanres.13512.

19. Park, H.-J.; Kim, M.-M. Amentoflavone Induces Autophagy and Modulates P53. Cell J. 2018, 21, 27–34, doi:10.22074/cellj.2019.5717.

20. Pei, J.-S.; Liu, C.-C.; Hsu, Y.-N.; Lin, L.-L.; Wang, S.-C.; Chung, J.-G.; Bau, D.-T.; Lin, S.-S. Amentoflavone Induces Cell-Cycle Arrest and Apoptosis in MCF-7 Human Breast Cancer Cells via Mitochondria-Dependent Pathway. Vivo 2012, 26, 963–970.

21. Siveen, K.S.; Kuttan, G. Effect of Amentoflavone, a Phenolic Component from Biophytum Sensitivum, on Cell Cycling and Apoptosis of B16F-10 Melanoma Cells. J. Environ. Pathol. Toxicol. Oncol. 2011, 30, 301–309, doi:10.1615/JEnvironPatholToxicolOncol.v30.i4.30.

22. Latunde-Dada, G.O. Ferroptosis: Role of Lipid Peroxidation, Iron and Ferritinophagy. Biochim. Biophys. Acta 2017, 1861, 1893–1900, doi:10.1016/j.bbagen.2017.05.019.

23. Gao, M.; Monian, P.; Pan, Q.; Zhang, W.; Xiang, J.; Jiang, X. Ferroptosis Is an Autophagic Cell Death Process. Cell Res. 2016, 26, 1021–1032, doi:10.1038/cr.2016.95.

24. Hou, W.; Xie, Y.; Song, X.; Sun, X.; Lotze, M.T.; Zeh, H.J.; Kang, R.; Tang, D. Autophagy Promotes Ferroptosis by Degrada-tion of Ferritin. Autophagy 2016, 12, 1425–1428, doi:10.1080/15548627.2016.1187366.

25. Chen, Y.; Mi, Y.; Zhang, X.; Ma, Q.; Song, Y.; Zhang, L.; Wang, D.; Xing, J.; Hou, B.; Li, H.; et al. Dihydroartemis-inin-Induced Unfolded Protein Response Feedback Attenuates Ferroptosis via PERK/ATF4/HSPA5 Pathway in Glioma Cells. J. Exp. Clin. Cancer Res. 2019, 38, 402, doi:10.1186/s13046-019-1413-7.

26. Du, J.; Wang, T.; Li, Y.; Zhou, Y.; Wang, X.; Yu, X.; Ren, X.; An, Y.; Wu, Y.; Sun, W.; et al. DHA Inhibits Proliferation and Induces Ferroptosis of Leukemia Cells through Autophagy Dependent Degradation of Ferritin. Free Radic. Biol. Med. 2019, 131, 356–369, doi:10.1016/j.freeradbiomed.2018.12.011.

27. Zhu, H.-Y.; Huang, Z.-X.; Chen, G.-Q.; Sheng, F.; Zheng, Y.-S. Typhaneoside Prevents Acute Myeloid Leukemia (AML) through Suppressing Proliferation and Inducing Ferroptosis Associated with Autophagy. Biochem. Biophys. Res. Commun. 2019, 516, 1265–1271, doi:10.1016/j.bbrc.2019.06.070.

28. Chen, G.-Q.; Benthani, F.A.; Wu, J.; Liang, D.; Bian, Z.-X.; Jiang, X. Artemisinin Compounds Sensitize Cancer Cells to Fer-roptosis by Regulating Iron Homeostasis. Cell Death Differ. 2020, 27, 242–254, doi:10.1038/s41418-019-0352-3.

29. Wang, K.; Zhang, Z.; Wang, M.; Cao, X.; Qi, J.; Wang, D.; Gong, A.; Zhu, H. Role of GRP78 Inhibiting Artesunate-Induced Ferroptosis in KRAS Mutant Pancreatic Cancer Cells. Drug Des. Dev. 2019, 13, 2135–2144, doi:10.2147/DDDT.S199459.

30. Eling, N.; Reuter, L.; Hazin, J.; Hamacher-Brady, A.; Brady, N.R. Identification of Artesunate as a Specific Activator of Fer-roptosis in Pancreatic Cancer Cells. Oncoscience 2015, 2, 517, doi:10.18632/oncoscience.160.

31. Greenshields, A.L.; Shepherd, T.G.; Hoskin, D.W. Contribution of Reactive Oxygen Species to Ovarian Cancer Cell Growth Arrest and Killing by the Anti-Malarial Drug Artesunate: Impact of Artesunate on Ovarian Cancer. Mol. Carcinog. 2017, 56, 75–93, doi:10.1002/mc.22474.

32. Roh, J.-L.; Kim, E.H.; Jang, H.; Shin, D. Nrf2 Inhibition Reverses the Resistance of Cisplatin-Resistant Head and Neck Cancer Cells to Artesunate-Induced Ferroptosis. Redox Biol. 2017, 11, 254–262, doi:10.1016/j.redox.2016.12.010.

33. Ishikawa, C.; Senba, M.; Mori, N. Evaluation of Artesunate for the Treatment of Adult T-Cell Leukemia/Lymphoma. Eur. J. Pharmacol. 2020, 872, 172953, doi:10.1016/j.ejphar.2020.172953.

34. Schröder, M.; Kaufman, R.J. ER Stress and the Unfolded Protein Response. Mutat. Res. 2005, 569, 29–63, doi:10.1016/j.mrfmmm.2004.06.056.

35. Xu, C. Endoplasmic Reticulum Stress: Cell Life and Death Decisions. J. Clin. Investig. 2005, 115, 2656–2664, doi:10.1172/JCI26373.

36. Wang, N.; Zeng, G.-Z.; Yin, J.-L.; Bian, Z.-X. Artesunate Activates the ATF4-CHOP-CHAC1 Pathway and Affects Ferroptosis in Burkitt's Lymphoma. Biochem. Biophys. Res. Commun. 2019, 519, 533–539, doi:10.1016/j.bbrc.2019.09.023.

37. Kumar, A.; Tikoo, S.; Maity, S.; Sengupta, S.; Sengupta, S.; Kaur, A.; Kumar Bachhawat, A. Mammalian Proapoptotic Factor ChaC1 and Its Homologues Function as Γ-glutamyl

Cyclotransferases Acting Specifically on Glutathione. EMBO Rep. 2012, 13, 1095–1101, doi:10.1038/embor.2012.156.

38. Crawford, R.R.; Prescott, E.T.; Sylvester, C.F.; Higdon, A.N.; Shan, J.; Kilberg, M.S.; Mungrue, I.N. Human CHAC1 Protein Degrades Glutathione, and MRNA Induction Is Regulated by the Transcription Factors ATF4 and ATF3 and a Bipartite ATF/CRE Regulatory Element. J. Biol. Chem. 2015, 290, 15878–15891, doi:10.1074/jbc.M114.635144.
39. Kimata, Y.; Kohno, K. Endoplasmic Reticulum Stress-Sensing Mechanisms in Yeast and Mammalian Cells. Curr. Opin. Cell Biol. 2011, 23, 135–142, doi:10.1016/j.ceb.2010.10.008.
40. Zhu, G.; Lee, A.S. Role of the Unfolded Protein Response, GRP78 and GRP94 in Organ Homeostasis. J. Cell Physiol. 2015, 230, 1413–1420, doi:10.1002/jcp.24923.
41. Yang, W.S.; Stockwell, B.R. Synthetic Lethal Screening Identifies Compounds Activating Iron-Dependent, Nonapoptotic Cell Death in Oncogenic-RAS-Harboring Cancer Cells. Chem. Biol. 2008, 15, 234–245, doi:10.1016/j.chembiol.2008.02.010.
42. Siddiqui, A.D.; Piperdi, B. KRAS Mutation in Colon Cancer: A Marker of Resistance to EGFR-I Therapy. Ann. Surg Oncol. 2010, 17, 1168–1176, doi:10.1245/s10434-009-0811-z.
43. Shady, W.; Petre, E.N.; Vakiani, E.; Ziv, E.; Gonen, M.; Brown, K.T.; Kemeny, N.E.; Solomon, S.B.; Solit, D.B.; Sofocleous, C.T. Kras Mutation Is a Marker of Worse Oncologic Outcomes after Percutaneous Radiofrequency Ablation of Colorectal Liver Metastases. Oncotarget 2017, 8, 66117–66127, doi:10.18632/oncotarget.19806.
44. Dodson, M.; Castro-Portuguez, R.; Zhang, D.D. NRF2 Plays a Critical Role in Mitigating Lipid Peroxidation and Ferroptosis. Redox Biol. 2019, 23, 101107, doi:10.1016/j.redox.2019.101107.
45. Lu, K.; Alcivar, A.L.; Ma, J.; Foo, T.K.; Zywea, S.; Mahdi, A.; Huo, Y.; Kensler, T.W.; Gatza, M.L.; Xia, B. NRF2 Induction Supporting Breast Cancer Cell Survival Is Enabled by Oxidative Stress–Induced DPP3–KEAP1 Interaction. Cancer Res. 2017, 77, 2881–2892, doi:10.1158/0008-5472.CAN-16-2204.
46. Zhang, D.D. Mechanistic Studies of the Nrf2-Keap1 Signaling Pathway. Drug Metab. Rev. 2006, 38,769–789, doi:10.1080/03602530600971974.
47. Lau, A.; Villeneuve, N.; Sun, Z.; Wong, P.; Zhang, D. Dual Roles of Nrf2 in Cancer. Pharmacol. Res. 2008, 58, 262–270, doi:10.1016/j.phrs.2008.09.003.
48. Gañán-Gómez, I.; Wei, Y.; Yang, H.; Boyano-Adánez, M.C.; García-Manero, G. Oncogenic Functions of the Transcription Factor Nrf2. Free Radic. Biol. Med. 2013, 65, 750–764, doi:10.1016/j.freeradbiomed.2013.06.041.
49. Habib, E.; Linher-Melville, K.; Lin, H.-X.; Singh, G. Expression of XCT and Activity of System Xc− Are Regulated by NRF2 in Human Breast Cancer Cells in Response to Oxidative Stress. Redox

Biol. 2015, 5, 33–42, doi:10.1016/j.redox.2015.03.003.

50. Lewerenz, J.; Albrecht, P.; Tien, M.-L.T.; Henke, N.; Karumbayaram, S.; Kornblum, H.I.; Wiedau-Pazos, M.; Schubert, D.; Maher, P.; Methner, A. Induction of Nrf2 and XCT Are Involved in the Action of the Neuroprotective Antibiotic Ceftriaxone in Vitro. J. Neurochem. 2009, 111, 332–343, doi:10.1111/j.1471-4159.2009.06347.x.
51. Ye, P.; Mimura, J.; Okada, T.; Sato, H.; Liu, T.; Maruyama, A.; Ohyama, C.; Itoh, K. Nrf2- and ATF4-Dependent Upregula-tion of XCT Modulates the Sensitivity of T24 Bladder Carcinoma Cells to Proteasome Inhibition. Mol. Cell Biol. 2014, 34, 3421–3434, doi:10.1128/MCB.00221-14.
52. Agyeman, A.S.; Chaerkady, R.; Shaw, P.G.; Davidson, N.E.; Visvanathan, K.; Pandey, A.; Kensler, T.W. Transcriptomic and Proteomic Profiling of KEAP1 Disrupted and Sulforaphane-Treated Human Breast Epithelial Cells Reveals Common Expres-sion Profiles. Breast Cancer Res. Treat. 2012, 132, 175–187, doi:10.1007/s10549-011-1536-9.
53. Harada, N.; Kanayama, M.; Maruyama, A.; Yoshida, A.; Tazumi, K.; Hosoya, T.; Mimura, J.; Toki, T.; Maher, J.M.; Yama-moto, M.; et al. Nrf2 Regulates Ferroportin 1-Mediated Iron Efflux and Counteracts Lipopolysaccharide-Induced Ferroportin 1 MRNA Suppression in Macrophages. Arch. Biochem. Biophys. 2011, 508, 101–109, doi:10.1016/j.abb.2011.02.001.
54. Xu, T.; Ding, W.; Ji, X.; Ao, X.; Liu, Y.; Yu, W.; Wang, J. Molecular Mechanisms of Ferroptosis and Its Role in Cancer Therapy. J. Cell Mol. Med. 2019, 23, 4900–4912, doi:10.1111/jcmm.14511.
55. Sun, X.; Ou, Z.; Chen, R.; Niu, X.; Chen, D.; Kang, R.; Tang, D. Activation of the P62-Keap1-NRF2 Pathway Protects against Ferroptosis in Hepatocellular Carcinoma Cells: Hepatobiliary Malignancies. Hepatology 2016, 63, 173–184, doi:10.1002/hep.28251.
56. Fan, Z.; Wirth, A.-K.; Chen, D.; Wruck, C.J.; Rauh, M.; Buchfelder, M.; Savaskan, N. Nrf2-Keap1 Pathway Promotes Cell Proliferation and Diminishes Ferroptosis. Oncogenesis 2017, 6, e371, doi:10.1038/oncsis.2017.65.
57. Dixon, S.J.; Stockwell, B.R. The Hallmarks of Ferroptosis. Annu. Rev. Cancer Biol. 2019, 3, 35–54, doi:10.1146/annurev-cancerbio-030518-055844.
58. Kwon, M.-Y.; Park, E.; Lee, S.-J.; Chung, S.W. Heme Oxygenase-1 Accelerates Erastin-Induced Ferroptotic Cell Death. Onco-target 2015, 6, 24393–24403, doi:10.18632/oncotarget.5162.
59. Hassannia, B.; Wiernicki, B.; Ingold, I.; Qu, F.; Van Herck, S.; Tyurina, Y.Y.; Bayır, H.; Abhari, B.A.; Angeli, J.P.F.; Choi, S.M.; et al. Nano-Targeted Induction of Dual Ferroptotic Mechanisms Eradicates High-Risk Neuroblastoma. J. Clin. Investig. 2018, 128, 3341–3355, doi:10.1172/JCI99032.
60. Hassannia, B.; Logie, E.; Vandenabeele, P.; Vanden Berghe, T.; Vanden Berghe, W. Withaferin A: From Ayurvedic Folk Med-icine to Preclinical Anti-Cancer Drug. Biochem. Pharmacol. 2020, 173, 113602, doi:10.1016/j.bcp.2019.08.004.

61. Efimova, I.; Catanzaro, E.; Van der Meeren, L.; Turubanova, V.D.; Hammad, H.; Mishchenko, T.A.; Vedunova, M.V.; Fi-mognari, C.; Bachert, C.; Coppieters, F.; et al. Vaccination with Early Ferroptotic Cancer Cells Induces Efficient Antitumor Immunity. J. Immunother. Cancer 2020, 8, e001369, doi:10.1136/jitc-2020-001369.

62. Yang, W.S.; Stockwell, B.R. Synthetic Lethal Screening Identifies Compounds Activating Iron-Dependent, Nonapoptotic Cell Death in Oncogenic-RAS-Harboring Cancer Cells. Chem. Biol. 2008, 15, 234–245, doi:10.1016/j.chembiol.2008.02.010.

63. Siddiqui, A.D.; Piperdi, B. KRAS Mutation in Colon Cancer: A Marker of Resistance to EGFR-I Therapy. Ann. Surg Oncol. 2010, 17, 1168–1176, doi:10.1245/s10434-009-0811-z.

64. Shady, W.; Petre, E.N.; Vakiani, E.; Ziv, E.; Gonen, M.; Brown, K.T.; Kemeny, N.E.; Solomon, S.B.; Solit, D.B.; Sofocleous, C.T. Kras Mutation Is a Marker of Worse Oncologic Outcomes after Percutaneous Radiofrequency Ablation of Colorectal Liver Metastases. Oncotarget 2017, 8, 66117–66127, doi:10.18632/oncotarget.19806.

65. Dodson, M.; Castro-Portuguez, R.; Zhang, D.D. NRF2 Plays a Critical Role in Mitigating Lipid Peroxidation and Ferroptosis. Redox Biol. 2019, 23, 101107, doi:10.1016/j.redox.2019.101107.

66. Lu, K.; Alcivar, A.L.; Ma, J.; Foo, T.K.; Zywea, S.; Mahdi, A.; Huo, Y.; Kensler, T.W.; Gatza, M.L.; Xia, B. NRF2 Induction Supporting Breast Cancer Cell Survival Is Enabled by Oxidative Stress–Induced DPP3–KEAP1 Interaction. Cancer Res. 2017, 77, 2881–2892, doi:10.1158/0008-5472.CAN-16-2204.

67. Zhang, D.D. Mechanistic Studies of the Nrf2-Keap1 Signaling Pathway. Drug Metab. Rev. 2006, 38,769–789, doi:10.1080/03602530600971974.

68. Lau, A.; Villeneuve, N.; Sun, Z.; Wong, P.; Zhang, D. Dual Roles of Nrf2 in Cancer. Pharmacol. Res. 2008, 58, 262–270, doi:10.1016/j.phrs.2008.09.003.

69. Gañán-Gómez, I.; Wei, Y.; Yang, H.; Boyano-Adánez, M.C.; García-Manero, G. Oncogenic Functions of the Transcription Factor Nrf2. Free Radic. Biol. Med. 2013, 65, 750–764, doi:10.1016/j.freeradbiomed.2013.06.041.

70. Habib, E.; Linher-Melville, K.; Lin, H.-X.; Singh, G. Expression of XCT and Activity of System Xc− Are Regulated by NRF2 in Human Breast Cancer Cells in Response to Oxidative Stress. Redox Biol. 2015, 5, 33–42, doi:10.1016/j.redox.2015.03.003.

71. Lewerenz, J.; Albrecht, P.; Tien, M.-L.T.; Henke, N.; Karumbayaram, S.; Kornblum, H.I.; Wiedau-Pazos, M.; Schubert, D.; Maher, P.; Methner, A. Induction of Nrf2 and XCT Are Involved in the Action of the Neuroprotective Antibiotic Ceftriaxone in Vitro. J. Neurochem. 2009, 111, 332–343, doi:10.1111/j.1471-4159.2009.06347.x.

72. Ye, P.; Mimura, J.; Okada, T.; Sato, H.; Liu, T.; Maruyama, A.; Ohyama, C.; Itoh, K. Nrf2- and ATF4-Dependent Upregula-tion of XCT Modulates the Sensitivity of T24 Bladder Carcinoma Cells

to Proteasome Inhibition. Mol. Cell Biol. 2014, 34, 3421–3434, doi:10.1128/MCB.00221-14.

73. Agyeman, A.S.; Chaerkady, R.; Shaw, P.G.; Davidson, N.E.; Visvanathan, K.; Pandey, A.; Kensler, T.W. Transcriptomic and Proteomic Profiling of KEAP1 Disrupted and Sulforaphane-Treated Human Breast Epithelial Cells Reveals Common Expres-sion Profiles. Breast Cancer Res. Treat. 2012, 132, 175–187, doi:10.1007/s10549-011-1536-9.
74. Harada, N.; Kanayama, M.; Maruyama, A.; Yoshida, A.; Tazumi, K.; Hosoya, T.; Mimura, J.; Toki, T.; Maher, J.M.; Yama-moto, M.; et al. Nrf2 Regulates Ferroportin 1-Mediated Iron Efflux and Counteracts Lipopolysaccharide-Induced Ferroportin 1 MRNA Suppression in Macrophages. Arch. Biochem. Biophys. 2011, 508, 101–109, doi:10.1016/j.abb.2011.02.001.
75. Xu, T.; Ding, W.; Ji, X.; Ao, X.; Liu, Y.; Yu, W.; Wang, J. Molecular Mechanisms of Ferroptosis and Its Role in Cancer Therapy. J. Cell Mol. Med. 2019, 23, 4900–4912, doi:10.1111/jcmm.14511.
76. Sun, X.; Ou, Z.; Chen, R.; Niu, X.; Chen, D.; Kang, R.; Tang, D. Activation of the P62-Keap1-NRF2 Pathway Protects against Ferroptosis in Hepatocellular Carcinoma Cells: Hepatobiliary Malignancies. Hepatology 2016, 63, 173–184, doi:10.1002/hep.28251.
77. Fan, Z.; Wirth, A.-K.; Chen, D.; Wruck, C.J.; Rauh, M.; Buchfelder, M.; Savaskan, N. Nrf2-Keap1 Pathway Promotes Cell Proliferation and Diminishes Ferroptosis. Oncogenesis 2017, 6, e371, doi:10.1038/oncsis.2017.65.
78. Dixon, S.J.; Stockwell, B.R. The Hallmarks of Ferroptosis. Annu. Rev. Cancer Biol. 2019, 3, 35–54, doi:10.1146/annurev-cancerbio-030518-055844.
79. Kwon, M.-Y.; Park, E.; Lee, S.-J.; Chung, S.W. Heme Oxygenase-1 Accelerates Erastin-Induced Ferroptotic Cell Death. Onco-target 2015, 6, 24393–24403, doi:10.18632/oncotarget.5162.
80. Bebber, C.M.; Müller, F.; Prieto Clemente, L.; Weber, J.; von Karstedt, S. Ferroptosis in Cancer Cell Biology. Cancers 2020, 12, 164, doi:10.3390/cancers12010164.
81. Hassannia, B.; Logie, E.; Vandenabeele, P.; Vanden Berghe, T.; Vanden Berghe, W. Withaferin A: From Ayurvedic Folk Med-icine to Preclinical Anti-Cancer Drug. Biochem. Pharmacol. 2020, 173, 113602, doi:10.1016/j.bcp.2019.08.004.
82. Efimova, I.; Catanzaro, E.; Van der Meeren, L.; Turubanova, V.D.; Hammad, H.; Mishchenko, T.A.; Vedunova, M.V.; Fi-mognari, C.; Bachert, C.; Coppieters, F.; et al. Vaccination with Early Ferroptotic Cancer Cells Induces Efficient Antitumor Immunity. J. Immunother. Cancer 2020, 8, e001369, doi:10.1136/jitc-2020-001369.